Pergamon

www.neuroscience-ibro.com

PII: S0306-4522(02)00145-8

Neuroscience Vol. 113, No. 1, pp. 125–135, 2002

0306-4522/02 $22.00+0.00

QUANTAL TRANSMITTER RELEASE BY GLIOMA CELLS: QUANTIFICATION OF INTRAMEMBRANE PARTICLE CHANGES

E. BUGNARD,[a] N. TAULIER,[b] A. BLOC,[a] P. CORRÈGES,[a] J. FALK-VAIRANT,[a] P. SORS,[a] F. LOCTIN[a] and Y. DUNANT[a]*

[a]Département de Pharmacologie, Centre Médical Universitaire, CH-1211 Genève 4, Switzerland

[b]Department of Pharmaceutical Sciences, Faculty of Pharmacy, University of Toronto, 19 Russell Street, Toronto, ON, Canada M5S 2S2

Abstract—Glial cells *in situ* are able to release neurotransmitters such as glutamate or acetylcholine (ACh). Glioma C6BU-1 cells were used to determine whether the mechanisms of ACh release by a glial cell line are similar or not to quantal release from neurones. Individual C6BU-1 cells, pre-filled with ACh, were moved into contact with a *Xenopus* myocyte that was used as a real-time ACh detector. Upon electrical stimulation, C6BU-1 cells generated evoked ACh impulses which were Ca^{2+}-dependent and quantal (quantal steps of ca. 100 pA). Changes in plasma membrane ultrastructure were investigated by using a freeze-fracture technique designed for obtaining large and flat replicas from monolayer cell cultures. A transient increase in the density of medium and large size intramembrane particles – and a corresponding decrease of small particles – occurred in the plasma membrane of C6BU-1 cells stimulated for ACh release. Changes in interaction forces between adjacent medium and large particles were investigated by computing the radial distribution function and the interaction potential. In resting cells, the radial distribution function revealed a significant increase in the probability to find two particles separated by an interval of 24 nm; the interaction potential suggested repulsive forces for intervals shorter than 24 nm and attractive forces between 24 and 26 nm. In stimulated cells, this interaction was displaced to 21 nm and made weaker, despite of the fact that the overall particle density increased. The nature of this transient change in intramembrane particles is discussed, particularly with regard to the mediatophore proteolipid which is abundant in the membranes C6-BU-1 like in those of cholinergic neurones. In conclusion, evoked ACh release from pre-filled C6-BU-1 glioma cells is quantal and Ca^{2+}-dependent. It is accompanied by a transient changes in the size distribution and the organisation of intramembrane particles in the plasma membrane. Thus, for the release characteristics, glioma cells do not differ fundamentally from neurones.

Key words: acetylcholine release, freeze-fracture morphology, intramembrane particles, mediatophore, pair distribution analysis, vesicle openings.

Glial cells of the central and peripheral nervous systems have been reported to play more than a merely supportive and trophic role. In vertebrates and invertebrates, they contain neurotransmitters such as acetylcholine (ACh) or glutamate and are believed to exert a modulation of synaptic transmission (Dennis and Miledi, 1974; Villegas and Jenden, 1979; Parri et al., 2001). However, the mechanisms of transmitter release by glial cells are still enigmatic. At the denervated neuromuscular junction, Schwann cells occupy the synaptic gutter and generate ACh quanta whose characteristics are, on several aspects, different from those of the classical quanta, produced by nerve terminals at normally innervated synapses (Dennis and Miledi, 1974; Kriebel et al., 1980). Glutamate release from astrocytes can be elicited by various agents (glutamate itself, prostaglandins, bradykinin) and is Ca^{2+}-dependent but resistant to tetanus toxin (Bezzi et al., 1998). This rises intriguing questions since glial cells do not exhibit the characteristic cytological differentiation of nerve terminals. Is the mechanism of release different in neurones and glial cells? Are the membrane changes accompanying transmitter release the same in glia and neurones?

Rat glioma C6-BU-1 cells (C6 cells) are particularly suited for addressing such questions. Although they do not express proteins of the cholinergic locus (choline acetyltransferase and the vesicular ACh transporter) they efficiently release ACh in a Ca^{2+}-dependent manner, as demonstrated by pre-filling the cells with the transmitter (Israël et al., 1994; Falk-Vairant et al., 1996b). Under these conditions, C6 cells release either ACh or GABA, but not glutamate (Israël et al., 1997). This might be surprising since C6 is regarded as an astrocytoma cell line, and astrocytes *in situ* efficiently release glutamate (Bezzi et al., 1998; Parri et al., 2001).

In the present study, we have further investigated the

*Corresponding author. Tel.: +41-22-702-54-32; fax: +41-22-702-54-52.

E-mail address: yves.dunant@medecine.unige.ch (Y. Dunant).

Abbreviations: ACh, acetylcholine; C6, glioma C6BU-1 cells; DMEM, Dulbecco's modified Eagle's medium; FCS, foetal calf serum; HEPES, *N*-(2-hydroxyethyl)piperazine-*N*′-(2-ethanesulphonic acid); IMP, intramembrane particle; P- or E-face, the cytoplasmic leaflet of the plasma membrane, respectively; PBS, phosphate-buffered saline.

quantal nature of ACh release from individual C6 cells in response to electrical stimulation, by using *Xenopus* myocytes as real-time ACh detectors. We have also measured ACh release from populations of C6 cells by using a calcium ionophore and a chemiluminescent assay. Monolayer cultures were fixed at different periods of time after the onset of stimulation and prepared for freeze-fracture morphology. Since we observed a transient alteration in the size distribution of intramembrane particles (IMPs), we submitted the membrane pictures to pair distribution analysis for determining whether reciprocal interaction exists between particles (most probably proteins) and whether these parameters are altered during activity. This work also afforded the opportunity to compare the mechanisms of ACh release taking place in C6 cells to those of neuronal cell lines or naturally occurring nerve terminals.

EXPERIMENTAL PROCEDURES

Cell culture

C6-BU-1 cells (provided by M. Israël, Gif-sur-Yvette, France) were cultured in Dulbecco's modified Eagle's medium (DMEM; Eurobio, France; Ca^{2+} concentration: 1.46 mM) supplemented with glutamine (2 mM) and 10% foetal calf serum (FCS). The cultures were carried out at 37°C in a 5% CO_2–95% air mixture saturated with water. To be filled with ACh, the cells were deprived of choline during 4 days before experiments. Twelve to 15 h before the release run, the cells were loaded with ACh (40 mM) in the presence of ecothiopate iodide (1 μM; a generous gift from Wyeth-Ayerst Pharmaceuticals, St. Davids, PA, USA). For morphological experiments, cultures were grown in monolayer until confluence on plastic coverslips (Thermanox®, Nunc, IL, USA).

Real-time detection of quantal ACh release

In brief, pre-filled C6 cells were harvested after trypsin treatment, extensively washed with choline-free DMEM and carefully laid down onto a culture of embryonic *Xenopus* myocytes. By using a fine-tipped glass micropipette (8–10 MΩ) filled with the extracellular solution, one C6 cell was then gently manipulated and placed into contact with a spherical myocyte. The same pipette was used to stimulate the glioma cell extracellularly (square pulses of 2 ms, 1–2 V, applied at 0.25 Hz). Whole-cell recordings were performed from the myocyte which was voltage-clamped at −70 mV and membrane currents were monitored by an Axopatch 200-A amplifier (Axon Instruments, Foster City, CA, USA). Signals, low-pass filtered at 1 or 5 kHz, were digitised on line at 2.5–10 kHz using a Lab-PC+ board (National Instruments, Austin, TX, USA) interfaced with a computer. Acquisition and off-line analysis were performed using the WCP software provided by J. Dempster (Strathclyde Electrophysiology Software, Glasgow, Scotland). Unless indicated, all recordings were made at room temperature in a solution containing (in mM): 140 NaCl, 3 KCl, 2 $CaCl_2$, 1 $MgCl_2$, 20 D-glucose, and 10 HEPES (pH 7.3). The internal solution in the patch pipettes contained (in mM): 150 KCl, 1 NaCl, 1 $MgCl_2$, and 10 HEPES (pH 7.2). The pipettes filled with this solution had an open resistance of 3–5 MΩ, and access resistance was kept below 10 MΩ. For more details see Falk-Vairant et al. (1996a) and Bloc et al. (1999).

Biochemical detection of ACh release

ACh release was monitored by using the choline oxidase chemiluminescence procedure (Israël and Lesbats, 1981; Israël et al., 1994). After four washings with DMEM lacking choline and FCS, and harvesting by trypsin treatment, a cell suspension volume corresponding to 10^5 cells was added to the chemiluminescent reaction mixture. The calcium ionophore A23187 (6 μM; Calbiochem, Lucerne, Switzerland) was then applied, followed by the addition of Ca^{2+} (10 mM final concentration) which triggered transmitter release. The ionophore could also be given after or together with Ca^{2+}, resulting in the same release kinetics. Subsequently, standard doses of ACh were added in the same vial to calibrate the amount released.

Stimulation of ACh release in morphological experiments

Experiments were carried out at room temperature with continuous and slow shaking. The culture medium was replaced by fresh DMEM lacking choline and FCS. To elicit release, the cultures were stimulated *in situ* by addition of the calcium ionophore A-23187 (6 μM) and Ca^{2+} (10 mM final concentration). Controls were treated with the same Ca^{2+} concentration but A23187 was omitted. At appropriate times, the cultures were progressively fixed by replacing the medium with a large volume of 4% paraformaldehyde in phosphate-buffered saline (PBS). After 2 h fixation at room temperature, the cultures were washed three times 5 min in PBS.

Flatten-peeled and freeze-fracture procedures

This method (Corrèges et al., 1996), provides freeze-fracture replicas exposing large and homogeneous areas of membrane cytoplasmic leaflet (P)-faces, which is very convenient for morphometric analysis (Bugnard et al., 1998). The monolayer grown on a Thermanox® coverslip was flattened in a sandwich consisting of a piece of Falcon® membrane (Falcon Cell Culture Insert 3090; Becton Dickinson, Wohlen, Switzerland) and a glass coverslip. The sandwich was placed overnight in a closed humid chamber at 4°C with a weight of about 5 g on the upper coverslip. The day after, the sandwich was separated and the coverslip with the attached and flattened monolayer was immersed in a solution of 30% glycerol/70% PBS (w/v) for 1 h. The coverslip was cut into squares of ca. 1 mm^2 which were attached with vinol on a gold carrier designed to be fitted onto the stage of the freeze-fracture apparatus. The assembly was frozen in a mixture of 90% propane and 10% isopentane maintained at −180°C with liquid nitrogen. Freeze fracture was achieved by peeling the membrane in a Balzers freeze-etch unit (BAF 300, Balzers AG, Balzers, Lichtenstein). Temperature was set at −100°C and pressure at 10^{-7} mbar. The Balzers knife blade was placed beneath the coverslip to which the cell culture was attached. The coverslip was removed by raising the blade slowly without touching the monolayer of cells. Reproducible replicas were obtained by evaporating 2 nm of platinum and 20 nm of carbon applied at 45° and 90°, respectively. The replicas were detached from the gold carrier by immersion in a filtered solution of hypochloride (42.3 g/l) during 20 min. Then, the replicas were skimmed with a solution of 1/3 methanol–2/3 chloroform for 20 min. The liquid was aspirated, leaving the replicas in the bottom of the receptacle. To catch the replicas, distilled water was slowly added, making them to float. Each replica was laid down on a 300 mesh copper grid (TEBRA 1GC400), dried, examined and photographed with a transmission electron microscope at 80 kV (Philips CM10, Philips, Eindhoven, Netherlands).

Morphometric analysis

For each condition, three cultures were proceeded and several regions were randomly photographed. IMPs and pits (vesicle openings) were quantified by three workers in a blind test protocol. The IMPs were counted within squares corresponding to 1 μm^2, on transparent sheets superimposed on the photographs at a magnification of 34 000. For each condition, 10 squares of 1 μm^2 were taken from five different cell membrane areas. The number of small, middle size and large IMPs was evaluated on

the squares by comparison with 'standard' IMPs drawn on the transparent sheet. In addition, we have measured more directly the diameter of at least 120 individual IMPs taken from five different areas in four experimental conditions. The IMP diameter was measured as the length of a line drawn at the base of the triangular shadow projected by the particle, perpendicular to the direction of the shadowing. Pits (vesicle openings) were counted in a blind manner by three persons on 10 areas of 23.75 μm^2 for each condition at a magnification of 13 500. For quantitative analysis, the flatness of replicas and the quality of shadowing were the only criteria of choice. The Student's unpaired *t*-test was used to determine the significance of differences between the values of data groups.

Pair distribution function and interaction potential

By definition, the pair distribution function $g(r)$ is the ratio of the IMP density $P(r)$ in an annulus defined by radii r and $(r+\Delta r)$ centred on a given particle, to ρ, the overall mean density of IMPs. Consequently, a $g(r)$ value larger than 1 at a given interval, means that the density of particles is locally higher than the overall mean IMP density. Conversely, at a distance where $g(r)$ is smaller than 1, the IMP density is lower than the overall mean density. The difficulty of calculating $g(r)$ resides in the determination of $P(r)$, which need the knowledge of the co-ordinates of all proteins. To that end, the position of all IMPs with a diameter ≥ 10 nm was marked on a transparent sheet superimposed to photographs of the freeze-fracture replicas (magnification: 100 000). This was done for the two experimental conditions which exhibited the most significant IMP changes. Namely, we analysed 1 μm^2 squares of 10 P-face replicas from different resting cells (908 IMPs) and of height P-face replicas from different 'releasing' cells (1741 IMPs), that is, from cultures whose fixation started at 10 s after Ca^{2+} application. IMP co-ordinates were then obtained by digitising the transparent sheets containing the particle positions.

Another useful function is the pair correlation function $[g(r)-1]$, which measures the correlation between two proteins separated by a distance r. This function can be divided into a sum of a direct contribution, $c(r)$, and an indirect contribution due to a third particle located at r': $g(r)-1 = c(r)+\rho\int c(r')[g(r')-1]dr'$, which is called the Orstein–Zernike (OZ) equation (Ornstein and Zernike, 1914). The interaction potential, $u(r)$, is then related to $c(r)$ through the Percus–Yevick (PY) equation (Percus and Yevick, 1958): $c(r) = g(r)(1-e^{u(r)}/_{k_B T})$. As a consequence, the interaction potential can be derived from $g(r)$ by solving the OZ and PY equations, by using the algorithm of Lado (1968).

RESULTS

Quantal ACh release from pre-filled C6 cells

Under the present experimental conditions, the glioma C6 cells grew easily in culture, became elongated and formed a network when approaching confluence (Fig. 1A). Cells in monolayer culture were pre-filled overnight by incubation in the presence of 40 mM ACh. They were subsequently washed, resuspended and transmitter release was elicited by application of Ca^{2+} in the presence of the calcium ionophore A23187. The time course of release was monitored by the light trace of the luminescence reaction. The release rate was maximum about 2 min after Ca^{2+} application. Then it subsided (Fig. 1B). Control cells, treated with the same Ca^{2+} concentration (10 mM) in the absence of A23187, did not release any ACh. This was a first way to demonstrate that ACh release by C6 cells is Ca^{2+}-dependent. A similar protocol was used to stimulate the C6 cultures in the morphological experiments described below.

Individual cells, pre-filled with ACh, were moved into contact with a voltage-clamped embryonic *Xenopus* myocyte. Evoked ACh release was elicited from the C6 cell by brief depolarising pulses, and recorded in real-time from the myocyte as rapid inward currents. Under these conditions, a glioma cell can generate 20–50 responses. In many cases, the amplitude of the currents progressively declined as a function of time. Under favourable conditions, the amplitude fluctuated around a constant mean level. In these cases the responses exhibited discrete preferential steps, showing that ACh release from the C6 cell is quantal (Fig. 1C). The evoked currents resulted from the nicotinic action of ACh quanta on the myocyte receptors since tubocurarine (10 μM) abolished the responses (not illustrated). The Ca^{2+}-dependency of this evoked quantal release was assessed by temporarily perfusing the preparation with solution containing a high Mg^{2+} concentration and no added Ca^{2+}. As seen in Fig. 1D, evoked ACh release was abolished in Ca^{2+}-free medium.

Changes found in freeze-fracture replicas of C6 cell membranes

Large and flat areas of plasma membrane P-faces were obtained in the freeze-fracture replicas from C6 cultures submitted to the 'flatten-pealed' procedure. In control cells, pits of 40–70 nm diameter, most probably corresponding to vesicle openings, were encountered at a low frequency (approximately 1 per 10 μm^2). In addition, the P-faces were populated by a host of IMPs of various sizes (623 ± 11 per μm^2). Based on previous work on synapses *in situ* (Garcia-Segura et al., 1986) and neural cell cultures (Bugnard et al., 1999), we have divided IMPs into three classes: (i) large IMPs, with a diameter larger than 12.38 nm, (ii) medium size IMPs, ranging from 9.9 to 12.38 nm, and (iii) small IMPs with a diameter inferior to 9.9 nm. In control cells, the large IMPs were the minority (5%) while the small IMPs represented the prevailing population (66%; Figs. 2 and 3). The relative proportion of each class was fairly constant from one cell to another. Also the IMP density appeared to be relatively homogenous over these P-face areas. We did not notice 'specialised zones' in this respect.

To evaluate the changes accompanying and following ACh release, the cultures were stimulated by Ca^{2+} application in the presence of the ionophore A23189 and the fixative was applied at different times after Ca^{2+} addition. It should be stressed here that physiological processes are only slowly arrested during chemical fixation. While the luminometer trace gives a faithful image of the time course of ACh release (Fig. 1B), the times indicated for morphology are the times when the fixative was applied to the cultures. It certainly took 1–2 min until the membrane and intracellular processes could be arrested by chemical fixation (Buckley, 1973; Smith and Reese, 1980). We choose a chemical fixation in the present work chiefly because it afforded the use of the flatten-peeled procedure which provided unrivalled repli-

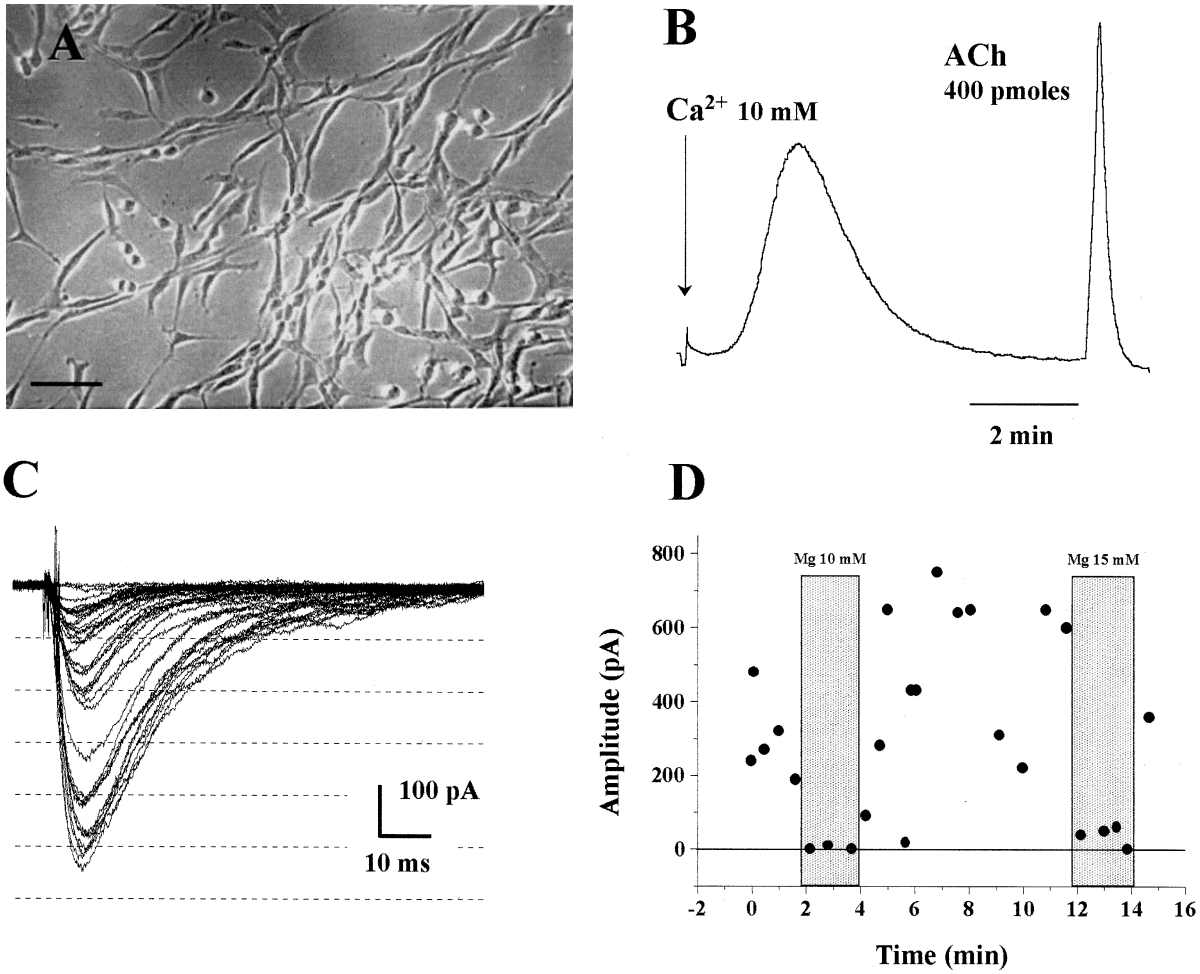

Fig. 1. Ca^{2+}-dependent and quantal ACh release by pre-filled glioma C6-BU-1 cells. (A) C6 cells in culture at the stage used for the release assay and for morphological experiments. Scale bar = 100 μm. (B) ACh release monitored by using the chemiluminescent reaction (Israël et al., 1994). Approximately 10^{-5} cells, pre-filled with ACh, were washed and resuspended in a medium containing the ingredients for the luminescence reaction. Then, the calcium ionophore A23187 (6 μM) was added to the mixture, followed by 10 mM $CaCl_2$ (arrow). The time course of ACh release was detected as an increase in luminescence. Standard doses of ACh were subsequently given to calibrate the response. (C) Evoked ACh release by a C6 cell pre-filled with the transmitter. The cell was stimulated by depolarising pulses (2 ms, 1 V, 0.25 Hz) applied through an external electrode. ACh release was detected by a *Xenopus* myocyte, voltage-clamped at −70 mV and placed in close contact with the C6 cell. The rapid inwards currents arose from activation of myocyte nicotinic receptors by the ACh quanta released from the glioma cell in response to electrical stimulation. In the picture, they were superimposed on the stimulation artefact. The evoked currents peaked at preferred amplitudes separated by approximately 100-pA intervals (see dotted lines). (D) In a similar experiment, the amplitude of the myocyte current has been plotted as a function of time. The C6 cell was given occasional electrical stimuli at the times indicated by the responses. All responses have been shown in the picture, including one 'failure'. During the two periods indicated, the external medium was replaced by a solution containing no added Ca^{2+} and the mentioned concentrations of Mg^{2+}. As a result, release was inhibited. Between these periods the current amplitude exhibited quantal fluctuations like in (C).

cas for morphometric analysis. On the other hand, this hindered us to determine the actual time course of membrane changes (see Discussion).

A dramatic change affected IMPs in cells that were submitted to the fixative from 10 s after Ca^{2+} application (fixation proceeding during the first 1–2 min). The total number of IMPs was not significantly modified at this stage (645 ± 15 IMPs per μm^2) but their size distribution was markedly altered (Fig. 2). At the 10-s point, the large IMPs and still more the 10–11-nm IMPs (medium class) greatly increased in number. For this period, the middle class transiently became the most abundant population. On the other hand, the density of the small IMPs decreased in proportion of the rise of middle size IMPs (Fig. 3). This occurred quite homogeneously on the whole surface of membrane replicas, without 'active zones' formation. The IMP change occurring during this initial period was highly significant, but it was transient. When fixation was started at 30 s or later, the proportion of large and medium size IMPs returned toward control values while the small IMPs became again the prevalent population. Some damped oscillation of IMP size distribution occurred during the recovery phase. Strikingly, during the whole course of the experiment, the curve describing the small IMPs density was practically the mirror image of that of middle size IMPs.

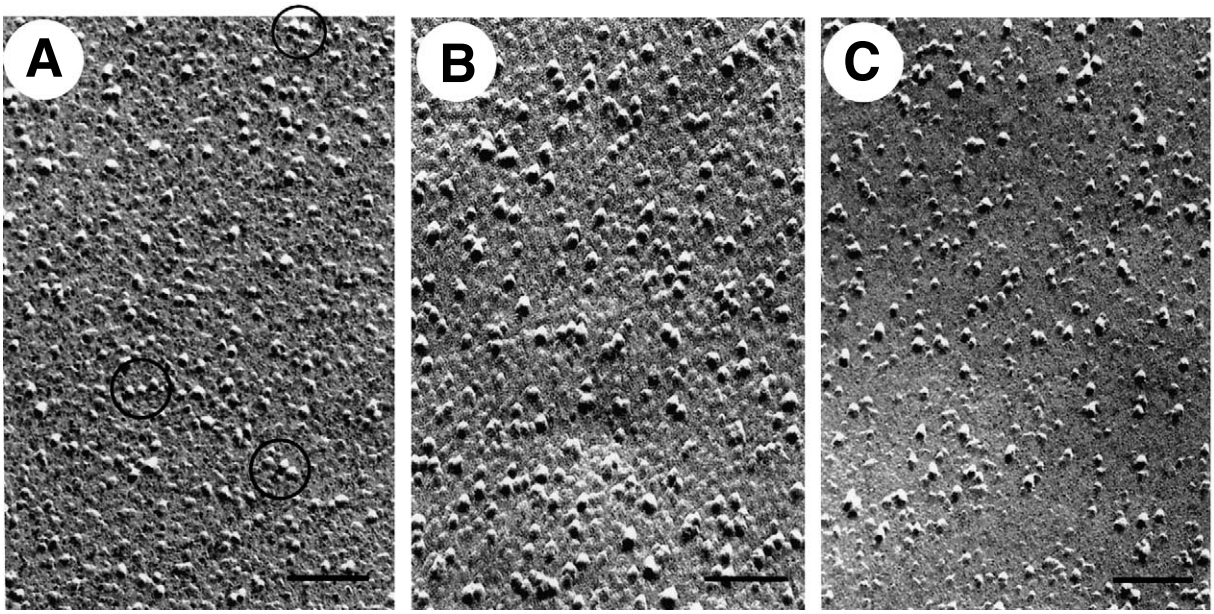

Fig. 2. Freeze-fracture replicas of the P-face of C6 cells. In (A), the cells received $CaCl_2$ in the absence of A23187 (control cells, no ACh release). Particles larger than 10 nm showed a tendency to be associated in pairs or small strings with centre to centre distances close to the 23–24 nm of the radial distribution function (see circles). (B) Cells fixed during the initial phase of the release protocol (fixation starting 10 s after $CaCl_2$ application). Notice the marked increase in the number of medium and large size IMPs and the decrease of small IMPs. (C) Cells fixed at a late time of the release run (5 min after $CaCl_2$ application). Scale bars = 1 μm.

Again, the total number of IMPs was not significantly altered throughout the experiment.

In the above analysis, IMPs were simply distributed into three predetermined size classes. Although the results blindly obtained by the three observers displayed a very satisfying concordance (no more than 10% variation), we found it appropriate to work out a more precise description of the phenomenon by measuring individually the diameter of IMPs at four time periods of the release course (unstimulated controls, and cells whose fixation started at 10 s, 1 min and 5 min after Ca^{2+} application). Using this procedure, the number of IMPs counted was lower (120 or more per condition) but the measurement of diameters was more accurate than in the first procedure. The size distribution histograms obtained in this way (Fig. 4) confirmed the transient shift occurring at the initial phase. During this period, the IMP diameters showed a peak at 10–11 nm. In all other conditions, the small particles were the majority.

We also counted in the replicas the number of pits (vesicle openings) present in the P-face of C6 cells. The density of pits remained constant in the membrane of cells which were given the fixative at 10, 30 and 60 s after Ca^{2+} application. Thus, the marked IMP alteration happening in the initial period of time was not accompanied by any significant change in pit occurrence. An increase in pit density was seen later on (fixation starting at 2.5 min) but was not statistically significant (Fig. 3). At this time, the distribution of pits displayed rather important variability from one area to another in the same P-face replicas. Some cells displayed large P-face surfaces devoid of pits; in other cells, quite a number of regular 50-μm pits were grouped in confined areas.

Control cells (resting condition) in the above results were those submitted to the Ca^{2+} challenge in the absence A23187. We checked in the luminescence experiments that no ACh release was elicited under these conditions. Previous work using releasing and non-releasing cells showed that A23187 *per se* (without Ca^{2+}) did not produce significant pit or IMP changes in the membranes (Bugnard et al., 1999).

Pair distribution function and interaction potential between IMPs

The IMP changes observed during the initial period of the experiments suggested some transient remodelling affecting intramembrane proteins at this stage. This raised important questions concerning the organisation of proteins in the plan of the membrane, principally: whether there are interactions between neighbouring IMPs, and whether these interactions change during activity.

The radial distribution function $g(r)$ and the interaction potential $u(r)$ of particles ≥ 10 nm were determined on replicas for the two most characteristic conditions, that is for resting cells and for those exhibiting the highest IMP change (fixation starting at 10 s after Ca^{2+} application). Results are illustrated in Fig. 5. At rest, the $g(r)$ function showed a peak for an inter-particle distance of 24 nm. Thus, 24 nm represented a preferential mean distance between the centre of two neighbour IMPs. Since the negative derivative of the interaction potential $u(r)$ is the force $F(r) = -du(r)/dr$, we conclude that the decreasing values exhibited by $u(r)/k_B T$ for intervals shorter than 24 nm indicate repulsive forces (i.e. $F(r) > 0$) between particles. Beyond this minimum the interaction potential increased, suggesting attractive

forces (i.e. $F(r) < 0$). The 24-nm interval could therefore be taken as equilibrium distance between repulsive and attractive forces (i.e. $F(r) = 0$).

In replicas from 'active' cells (fixation starting at the 10-s point), the density of the ≥ 10 nm IMPs increased markedly (see above) and the profile of $g(r)$ was significantly altered. The position of the peak was shifted to a lower value (21 nm) and the amplitude of the variation was much reduced. Correspondingly, the interaction potential of stimulated specimens displayed a minimum at 21 nm. The general shape was maintained but the amplitude change at 21 nm was lower than the value found in resting cells at 24 nm. In other words, the distribution of IMPs in the plan of the membrane showed a reduced degree of reciprocal interaction during activity.

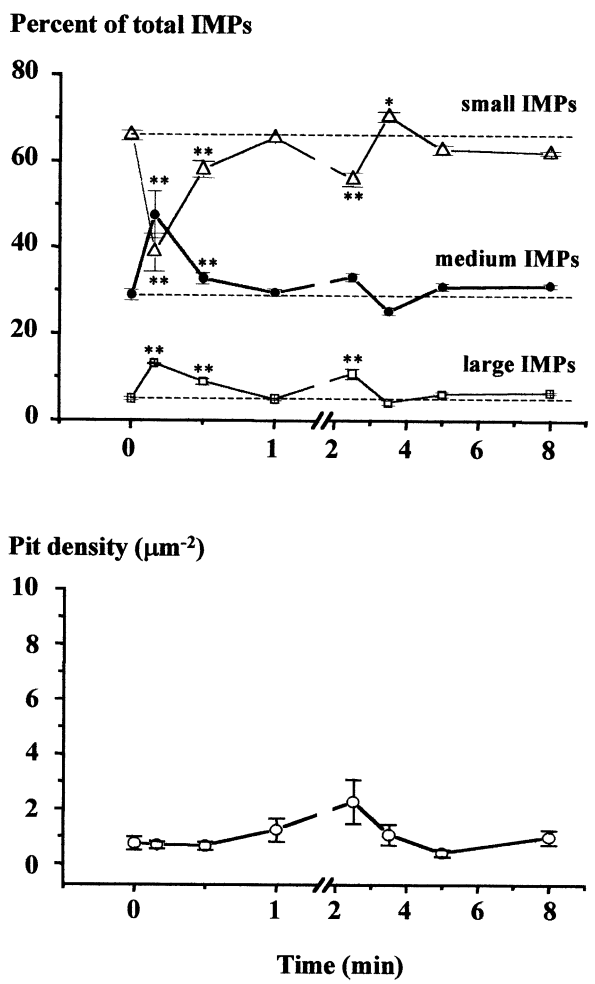

Fig. 3. Succession of morphological changes when the fixative was applied at different times during the course of the release experiments. (Top) Changes in the density of IMPs. Large, medium and small size IMPs are particles with a diameter >12.38 nm, 9.9–12.38 nm, and <9.9 nm, respectively. The proportion of the three IMP classes has been plotted here since the total number of particles did not change significantly (see text). Modifications of the small IMP density are the mirror image of those of the middle size IMPs. $*P < 0.05$, $**P < 0.01$, with respect to unstimulated cells, the values of which were indicated at the time ($t = 0$). (Bottom) Density of pits (vesicle openings) in the same replicas. The increase at 2.5 min was not statistically significant. As explained in the text, the times marked here are the times when the fixation solution was added to the cultures. The fixation itself proceeded only slowly after this time, probably taking 1–2 min.

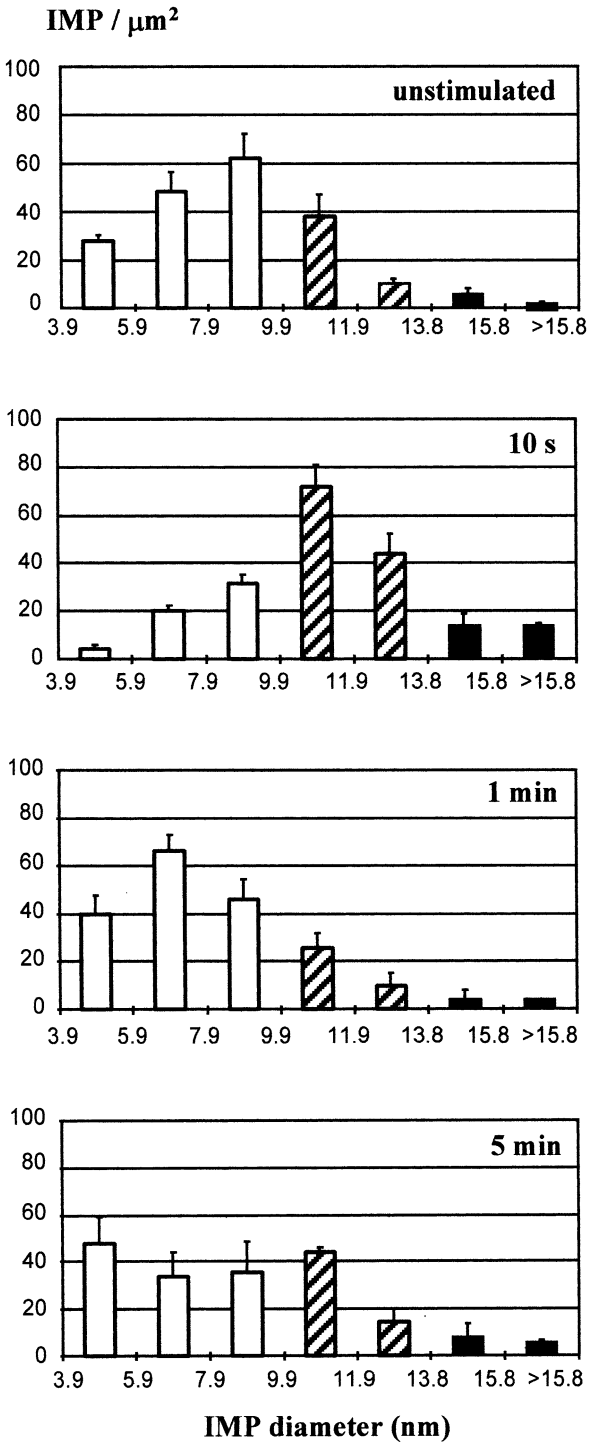

Fig. 4. Histograms of IMP diameters for the conditions indicated. The diameter of 120 or more particles per condition was measured as the length of a line drawn at the base of the shadow projected by the particle, perpendicular to the direction of the shadowing. The shift toward a larger IMP size is clearly seen in cells whose fixation began 10 s after Ca^{2+} application. The classes of small, medium and large IMPs (as defined for the large scale analysis of Fig. 3) are shown here using white, hatched and black histobars, respectively.

DISCUSSION

Calcium-dependency and quantal nature of ACh release by glioma cells

Schwann cells at the denervated neuromuscular junction were shown to release ACh in a quantal manner. However, the characteristics of the ACh quanta produced differ on several aspects from the classical quanta generated by nerve endings. The endplate potentials generated by Schwann cells occur at a low frequency: this frequency is rather reduced than increased by rising the Ca^{2+} concentration. In addition, their amplitude and time course exhibit large variations, with a majority of small quanta displaying a skewed size distribution (Birks et al., 1960; Kriebel and Gross, 1974; Kriebel et al., 1980; Colméus et al., 1982). In the present work, ACh was released in a clearly Ca^{2+}-dependent manner from pre-filled C6 cells, as demonstrated by using either the chemiluminescent assay, or the electrical stimulation combined to *Xenopus* myocyte real-time recording. One has to keep in mind, however, that the experimental conditions are quite different. At the denervated endplates, it was the spontaneous release that was observed while in the present experiments, Ca^{2+} was forced to enter the cells, either by electrical depolarisation or by an ionophore. With this type of stimulation, other types of neural and non-neural cells can also release ACh in a quantal manner (Falk-Vairant et al., 1996c).

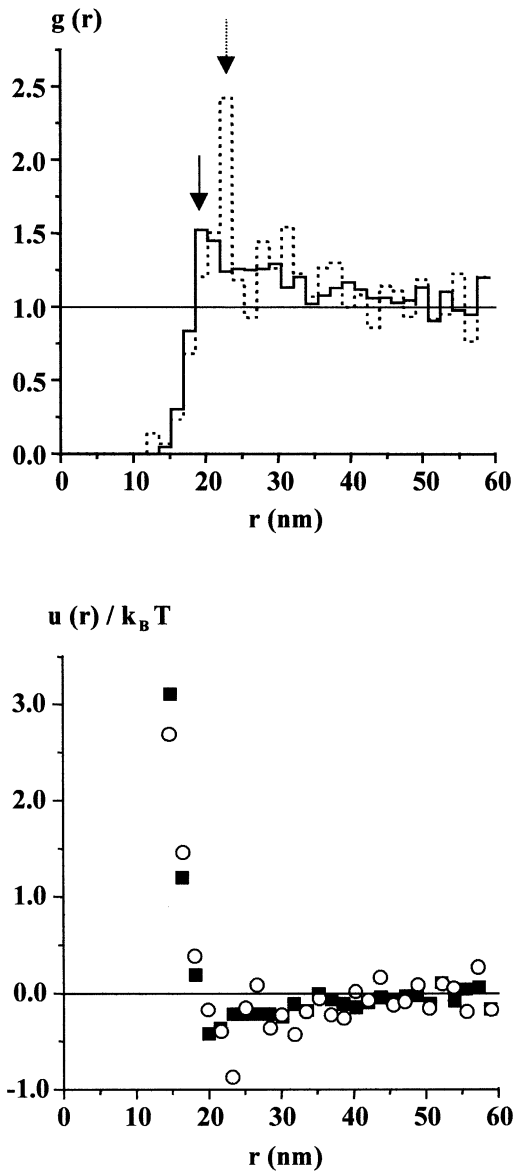

Fig. 5. Pair distribution function of IMP ≥ 10 nm in the P-face of glioma C6 cells, at rest and during the initial phase of the release run. In the replicas from control cells, the radial distribution function $g(r)$ reached a marked peak at $r = 24$ nm (dotted line, arrow). This means than particles situated at 23–24 nm from each other were significantly more numerous than expected from random distribution. Correspondingly, the interaction potential $u(r)/k_BT$ showed a minimum value for this interval (open circles). In stimulated cells, the peak of $g(r)$ was displaced to < 21 nm and had a lower amplitude (continuous line, arrow); the corresponding values of $u(r)/k_BT$ were displaced and attenuated (filled squares). Thus, the reciprocal interactions between medium and large IMPs were diminished during release, although their density was markedly increased. See further explanations in the text.

In the experiment illustrated in Fig. 1, the size of the quantal steps was close to 100 pA. Knowing that (i) opening of one *Xenopus* embryonic nicotinic receptor under the present conditions will generate a current of 1–2 pA (Kidokoro and Rohrbough, 1990), (ii) two ACh molecules are needed to activate one receptor, (iii) presumably more than half of the molecules are wasted in the process, the quanta recorded here should result from the synchronous release of at least 400 ACh molecules. This is much less than the 6000–10 000 molecules estimated for the full quantum in adult neuromuscular or nerve–electroplaque junctions (Kuffler and Yoshikami, 1975; Girod et al., 1993), but compares well with the values reported in embryonic endplates (Evers et al., 1989), sympathetic ganglia (Bennett, 1995), or in the population of small miniature currents which is believed to be the substructure of the classical quantum (Kriebel and Gross, 1974; Girod et al., 1993). A slightly larger value (200 pA) was obtained using neuroblastoma N18-TG-2 cells after transfection with the mediatophore, a proteolipid present in the presynaptic membrane cholinergic nerve terminals (Falk-Vairant et al., 1996a).

Thus, considering the elementary mechanism of quantal transmitter release and its Ca^{2+}-dependency, it may be hard to distinguish a 'neuronal mode' and a 'glial mode' of release (see Table 1). Probably the differences *in situ* result more from differences in the regulations of release, corresponding to well-known differences in cytological differentiation (different ion channels, involvement of synaptic vesicles, etc.).

Freeze-fracture morphology; IMPs and vesicle openings

The membrane changes accompanying and following ACh release were observed here in freeze-fracture replicas obtained from chemically fixed preparations. This approach has advantages and inconveniences. On the one hand, our main objective was to obtain reliable pictures for the above-described parametric analysis. Chemical fixation afforded the use of the flatten-peeled

Table 1. Characteristics of neurotransmitter release in glial and neuronal cells

	Glial cells *in situ*	Glial cell line (C6Bu-1) (present work)	Mediatophore transfected neuronal cell line (N18-TG-2)	Nerve terminals *in situ*
Ca^{2+}-dependency:				
evoked release	Yes[a]	Yes	Yes[e,f] (transfection required)	Yes[h]
spontaneous release	Not Ca^{2+}-dependent[b]	Extremely rare events	Extremely rare events	Yes (event frequency)
Quantal release	Yes[b,c] (skewed size distribution)	Yes (100-pA steps)	Yes[e,f] (transfection required) (200-pA steps)	Yes[i], quanta from 15 pA (SNC) to 2000 pA
Membrane changes accompanying release	N.D.	IMP changes	IMP changes[g] (transfection required), late pit occurrence	IMP changes, late pit occurrence[j–m]
Presence of mediatophore 15-kDa proteolipid in plasma membrane	N.D.	Yes[d]	Yes, but very low levels in non transfected cells[d,e]	Yes[n]

N.D., not determined to our knowledge.
[a]Bezzi et al., 1998.
[b]Kriebel et al., 1980.
[c]Dennis and Miledi, 1974.
[d]Israël et al., 1998.
[e]Falk-Vairant et al., 1996a.
[f]Bloc et al., 1999.
[g]Bugnard et al., 1999.
[h]Katz, 1969.
[i]Bennett, 1995.
[j]Garcia-Segura et al., 1986.
[k]Muller et al., 1987.
[l]Dunant, 2000.
[m]Heuser et al., 1979.
[n]Morel et al., 2001.

procedure which could provide the large and flat membrane areas we needed to this end. On the other hand, chemical fixation was shown to arrest physiological processes only slowly (Buckley, 1973; Smith and Reese, 1980). The cryofixation approach used previously to catch the real time course of synaptic events (Heuser et al., 1979; Garcia-Segura et al., 1986; Muller et al., 1987) would of course have given a much better time resolution, but it was less suitable for our purpose. Beyond this limitation, it was most important to determine whether the changes previously caught with rapid-freezing procedures could also be observed after chemical fixation. In the present set of results, chemical fixation must have caught the changes occurring during the first to second minutes following fixative application. It is therefore only the order of succession of events which is important to take into account here.

With this caveat in mind and on the basis of previous papers, it is reasonable to propose that the transient changes observed in cultures during the initial period after Ca^{2+} application (fixation starting at 10 s) corresponded to the release phase. A similar shift in time was observed under the same conditions in experiments using neuroblastoma cells (Bugnard et al., 1999). Moreover, the IMP changes reported here closely resembled the modifications previously found in other preparations, either chemically fixed or cryofixed. A marked increase in the density of medium and large IMPs, accompanied by a corresponding diminution of the small IMPs was reported for *Torpedo* synaptosomes quickly frozen during transmitter release (Israël et al., 1981) and in mammalian brain synaptosomes chemically fixed during KCl depolarisation in the presence of Ca^{2+} (Takano and Kamiya, 1979). An abrupt and fleeting rise in the density of medium and large IMPs has also been caught in the presynaptic membrane of rapidly frozen natural synapses during the precise time of release (Heuser et al., 1979; Garcia-Segura et al., 1986; Muller et al., 1987).

As for vesicle openings, the small increase observed in the present work was not significant. Stimulation of natural synapses results in an increase in the density of pits in the presynaptic membrane but, with one exception, i.e. the use of the 4-aminopyridine-treated neuromuscular junction (Heuser et al., 1979; Torri-Tarelli et al., 1985), the occurrence of vesicle openings was constantly delayed with regard to the very moment of transmitter release (see Table 1, and Dunant (2000) for a review).

Significance of the IMP changes

IMPs in replicas from living cells are generally believed to result from the presence of intrinsic membrane proteins (Branton, 1969), although IMPs were also demonstrated in artificial lipid membranes in the total absence of proteins (Verkleij, 1984). In a recent paper (Eskandari et al., 1998), a relation was found between the size of IMPs resulting from expression of known proteins in the oocyte membrane and the number of α-helices spanning in the plasmalemma. So, one α-helix would occupy 1.4 nm^2 of IMP surface. In our and other experiments the diameter of the transient IMP population arising during quantal ACh release was 10–12 nm and the thickness of the replica platinum film was approximately 2 nm. Thus, the protrusions causing such IMPs had a diameter

of approximately 6–8 nm and an area of 28.3–50.2 nm^2. This would correspond to 20–36 α-helices that would transiently appear inside the membrane. In this view, a peculiar protein would form only a small protrusion at rest – a small particle – in the interleaflet fracture plan. On activation, it would become more salient consecutively to some reorganisation or displacement of α-helices.

Other hypotheses could be put forward. The opposing changes in the number of small and middle size particles might suggest that membrane proteins momentarily form aggregates of a larger diameter when activated. A further proposal is that activation of releasing pores temporarily created hydrophilic sites inside the membrane. The water evaporated during the fracture process might recondensate on these hydrophilic spots and 'decorate' them (Gross et al., 1978).

Which protein could be concerned by the transient increase in the number of 10–12 nm IMPs? The integral membrane protein called mediatophore is a candidate. Mediatophore is an oligomer composed of a 15–16-kDa proteolipid, present at the active zone of the presynaptic cholinergic terminals. The 15 kDa proteolipid was shown to be much more abundant in the plasma membrane of C6 cells – which efficiently release ACh – than in the membranes of the neuroblastoma N18-TG-2 cells – which are not able to release pre-filled ACh (Israël et al., 1998). Reconstituted in various systems, mediatophore supports Ca^{2+}-dependent and quantal ACh release (Israël and Dunant, 1998). Moreover, IMPs were observed during ACh release in the membrane of proteoliposomes containing mediatophore as the unique protein (Brochier et al., 1992). Also, transfection of neuroblastoma N18-TG-2 cells with mediatophore cDNA induced both a Ca^{2+}-dependent and quantal ACh release (Falk-Vairant et al., 1996a; Bloc et al., 1999), and a transient increase of medium and large IMPs (Bugnard et al., 1999), as summarised in Table 1.

The 15-kDa proteolipid forming mediatophore is implicated in several cellular processes. It is a component of the membrane sector of V-ATPase (Nelson and Harvey, 1999); it was found in invertebrate gap junctions (Finbow and Pitts, 1998) and was recently identified in the yeast as the Ca^{2+}-sensitive proteolipid involved in membrane fusion (Peters et al., 2001). As suggested by the latter authors, it is possible that the proteolipid rings of 15-kDa subunits forming mediatophores expand radially during opening. At rest they would appear in freeze-fracture replicas as small IMPs, but when activated they would form 10–12 nm IMPs.

Pair distribution function of IMPs in the cell membrane

The objective of this quantitative analysis was to determine whether specific patterns of protein interaction occurred in the membrane and might parallel the IMP changes described here. The transient increase in density of the middle and large IMPs was accompanied by an important alteration of the pair distribution function, in particularly of the amplitude of the peak. Specifically, in replicas from unstimulated cells, the peak of the pair distribution exhibited a high value (ca. 2.5) for a distance 23–24 nm (Fig. 5), which means that a significant number of IMPs ≥ 10 nm were associated at this distance under the resting condition. Indeed, although there was no obvious inhomogeneity in the overall distribution of large IMPs in the plane of the membrane, often the particles tended to form pairs, or small strings or aggregates at a distance (centre to centre) of slightly more than 20 nm (see circles in Fig. 2A). Moreover, the interaction potentials in the resting conditions exhibited short-range repulsive interactions and strong long-range attractive interactions. The interval of 23–24 nm represented therefore an equilibrium point between attractive and repulsive forces. These patterns of interaction are not easy to interpret at the molecular level. They can result from direct interactions between proteins: electrostatic and van der Waals interactions (Israelachvili, 1985), attractive membrane-induced interactions due to membrane fluctuations (Park and Lubensky, 1996) or protein–membrane mismatch (Aranda-Espinoza et al., 1996). They can also arise from interactions involving the small IMPs. The latter were not included in the present analyses since many of them were at the limit of detection from the background granularity of the membrane picture and would be difficult to analyse accurately.

The interparticle association was lessened in the membrane of excited cells, that is, of cells fixed in the initial period after Ca^{2+} application. The peak of the distribution function reached then only the value of 1.5, indicating a looser interaction between the IMPs ≥ 10 nm, despite the fact that their density was increased. The general shape of the interaction potential was slightly modified after stimulation, which means that the interactions were only weakly modified during ACh release. However, the position of the minimum potential was shifted, indicating either a decrease in the repulsive interactions at short intervals, and the amplitude change was lessened suggesting a decrease in the attractive forces at more than 21 nm. It can be concluded that the interactions between adjacent particles were stronger at rest than during activation.

CONCLUSION

One of our objectives was to use C6 cells as a model to determine whether the mechanisms of ACh release could be fundamentally different between cells of glial or neuronal origin. Clearly, they were not, for the criteria investigated here (Table 1). Transmitter release from ACh-filled C6 glioma cells was quantal and Ca^{2+}-dependent, and was accompanied by a marked increase in the density of medium and large size IMPs in the plasma membrane. These three characteristics were also encountered in experiments using a neuroblastoma cell line transfected with the mediatophore 15-kDa proteolipid (which is also of neuronal origin: the electromotor nerve terminals of *Torpedo*). Moreover, Ca^{2+}-depedency, quantal behaviour, and transient IMP changes are all typical for ACh release in naturally occurring cholinergic terminals. Particularly, the transient IMP change was

observed in the presynaptic membrane during transmission of a single nerve impulse under the most physiological conditions (Muller et al., 1987). The C6 cells have provided an excellent system in the present work for initiating a parametric analysis of the fleeting IMP changes affecting the plasma membrane during transmitter release.

However, on several points the present approach allows only for limited conclusions. Chemical fixation precluded any faithful analysis of the time course of morphological events, and might have brought by itself modifications in the repartition of particles in the plan of the membrane. Also the external leaflet-faces of the plasma membrane could not be quantitatively examined although they might have been the site in interesting IMP changes. Finally the relationship between the 10–12 nm IMPs and mediatophore molecules could only be attempted on the basis of other works. To solve these questions, we have chosen to work again on the natural synapses *in situ*, by using in combination ultra-rapid freezing (Muller et al., 1987), labelled-fracture localisation of mediatophore proteolipid (Morel et al., 2001) and the above-described pair distribution analysis.

Acknowledgements—This work was supported by the Swiss National Foundation for Scientific Research (Grant No. 31 57135 99). We are grateful to F. Pillonel for the quality of the photographs. We want to thank M. Israël and N. Morel for useful advice and for providing the C6-BU-1 cell line.

REFERENCES

Aranda-Espinoza, H., Berman, A., Dan, N., Pincus, P., Safran, S., 1996. Interaction between inclusions embedded in membranes. Biophys. J. 71, 648–656.

Bennett, M.R., 1995. The origin of Gaussian distributions of synaptic potentials. Prog. Neurobiol. 46, 331–350.

Bezzi, P., Carmignoto, G., Pasti, L., Vesce, S., Rossi, D., Rizzini, B.L., Pozzan, T., Volterra, A., 1998. Prostaglandins stimulate calcium-dependent glutamate release in astrocytes. Nature 391, 281–285.

Birks, R.I., Katz, B., Miledi, R.B., 1960. Physiological and structural changes at the amphibian myoneural junction, in the course of degeneration. J. Physiol. Lond. 150, 145–168.

Bloc, A., Bugnard, E., Dunant, Y., Falk-Vairant, J., Israël, M., Loctin, F., Roulet, E., 1999. Acetylcholine synthesis and quantal release reconstituted by transfection of mediatophore and choline acetyltransferase cDNAs. Eur. J. Neurosci. 11, 1523–1534.

Branton, D., 1969. Membrane structure. Annu. Rev. Plant Physiol. 20, 206–238.

Brochier, G., Gulik-Krzywicki, T., Lesbats, B., Dedieu, J.C., Israël, M., 1992. Calcium-induced acetylcholine release and intramembrane particle occurrence in proteoliposomes equipped with mediatophore. Biol. Cell 74, 225–230.

Buckley, I.K., 1973. Studies on fixation for electron microscopy using cultured cells. Lab. Invest. 29, 398–410.

Bugnard, E., Sors, P., Bloc, A., Loctin, F., Dunant, Y., 1998. An improved approach to freeze-fracture morphology of monolayer cell cultures. J. Neurosci. Methods 82, 97–103.

Bugnard, E., Sors, P., Roulet, E., Bloc, A., Loctin, F., Dunant, Y., 1999. Morphological changes related to reconstituted acetylcholine release in a release-deficient cell line. Neuroscience 94, 329–338.

Colméus, C., Gomez, S., Molgo, J., Thesleff, S., 1982. Discrepancies between spontaneous and evoked synaptic potentials at normal, regenerating and botulinum toxin poisoned mammalian neuromuscular junctions. Proc. R. Soc. B. 215, 63–74.

Corrèges, P., Sors, P., Dunant, Y., 1996. Flatten-peeled: a new approach to freeze fracture morphology. Microsc. Res. Tech. 34, 478–487.

Dennis, M.J., Miledi, R.B., 1974. Characteristics of transmitter release at regenerating frog neuromuscular junctions. J. Physiol. Lond. 239, 571–594.

Dunant, Y., 2000. Quantal acetylcholine release: vesicle fusion or intramembrane particles? Microsc. Res. Tech. 49, 38–46.

Eskandari, S., Wright, E.M., Kreman, M., Starace, D.M., Zampighi, G.A., 1998. Structural analysis of cloned plasma membrane proteins by freeze-fracture electron microscopy. Proc. Natl. Acad. Sci. USA 95, 11235–11240.

Evers, J., Laser, M., Sun, Y., Xie, Z., Poo, M.M., 1989. Studies of nerve-muscle interactions in *Xenopus* cell culture: analysis of early synaptic currents. J. Neurosci. 9, 1523–1539.

Falk-Vairant, J., Corrèges, P., Eder-Colli, L., Salem, N., Roulet, E., Bloc, A., Meunier, F., Lesbats, B., Loctin, F., Synguelakis, M., Israël, M., Dunant, Y., 1996a. Quantal acetylcholine release induced by mediatophore transfection. Proc. Natl. Acad. Sci. USA 93, 5203–5207.

Falk-Vairant, J., Israël, M., Bruner, J., Stinnakre, J., Meunier, F.M., Gaultier, P., Meunier, F.A., Lesbats, B., Synguelakis, M., Corrèges, P., Dunant, Y., 1996b. Enhancement of quantal transmitter release and mediatophore expression by cyclic AMP in fibroblasts loaded with acetylcholine. Neuroscience 75, 353–360.

Falk-Vairant, J., Meunier, F.M., Lesbats, B., Corrèges, P., Eder-Colli, L., Salem, N., Synguelakis, M., Dunant, Y., Israël, M., 1996c. Cell lines expressing an acetylcholine release mechanism, correction of a release-defficient cell by mediatophore transfection. J. Neurosci. Res. 45, 195–201.

Finbow, M.E., Pitts, J.D., 1998. Structure of the ductin channel. Biosci. Rep. 18, 287–297.

Garcia-Segura, L.M., Muller, D., Dunant, Y., 1986. Increase in the number of presynaptic large intramembrane particles during synaptic transmission at the *Torpedo* nerve- electroplaque junction. Neuroscience 19, 63–79.

Girod, R., Corrèges, P., Jacquet, J., Dunant, Y., 1993. Space and time characteristics of transmitter release at the nerve-electroplaque junction of *Torpedo*. J. Physiol. Lond. 471, 129–157.

Gross, H., Kubler, O., Bas, E., Moor, H., 1978. Decoration of specific sites on freeze-fractured membrane. J. Cell Biol. 79, 646–656.

Heuser, J.E., Reese, T.S., Dennis, M.J., Jan, Y., Jan, L., Evans, L., 1979. Synaptic vesicle exocytosis captured by quick freezing and correlated with quantal transmitter release. J. Cell. Biol. 81, 275–300.

Israël, M., Dunant, Y., 1998. Acetylcholine release and the cholinergic genomic locus. Mol. Neurobiol. 16, 1–20.

Israël, M., Lesbats, B., 1981. Continuous determination by a chemiluminescent method of acetylcholine release and compartmentation in *Torpedo* electric organ synaptosomes. J. Neurochem. 37, 1475–1483.

Israël, M., Manaranche, R., Morel, N., Dedieu, J.C., Gulik-Krzywicki, T., Lesbats, B., 1981. Redistribution of intramembrane particles related to acetylcholine release by cholinergic synaptosomes. J. Ultrastruct. Res. 75, 162–178.

Israël, M., Lesbats, B., Synguelakis, M., Joliot, A., 1994. Acetylcholine accumulation and release by hybrid NG108-15, glioma and neuroblastoma cells – role of a 16 kDa membrane protein in release. Neurochem. Int. 25, 103–109.

Israël, M., Lesbats, B., Tomasi, M., Couraud, P.O., Vignais, L., Quinonéro, J., Tchélingérian, J.L., 1997. Calcium-dependent release specificities of various cell lines loaded with different transmitters. Neuropharmacology 36, 1789–1793.
Israël, M., Lesbats, B., Tomasi, M., Ohkuma, S., 1998. Enhanced acetylcholine release from cells that have more 15 kDa proteolipid in their membrane, a constituent of V-ATPase and mediatophore. J. Neurochem. 71, 630–635.
Israelachvili, J., 1985. Intermolecular and Surface Forces, 2nd edn. Academic, New York.
Katz, B., 1969. The Release of Neural Transmitter Substances. University, Liverpool, 60 pp.
Kidokoro, Y., Rohrbough, J., 1990. Acetylcholine receptor channels in *Xenopus* myocyte culture; brief openings, brief closures and slow desensitization. J. Physiol. Lond. 425, 227–244.
Kriebel, M.E., Gross, C.E., 1974. Multimodal distribution of frog miniature endplate potentials in adult, denervated and tadpole leg muscle. J. Gen. Physiol. 64, 85–103.
Kriebel, M.E., Hanna, R.B., Pappas, G.D., 1980. Spontaneous potentials and fine structure of identified frog denervated neuromuscular junctions. Neuroscience 5, 97–108.
Kuffler, S.W., Yoshikami, D., 1975. The number of transmitter molecules in a quantum: an estimate from iontophoretic application of acetylcholine at the neuromuscular synapse. J. Physiol. Lond. 251, 465–482.
Lado, F., 1968. Equations of state of the hard-disk fluid from approximate integral equations. J. Chem. Phys. 49, 3092–3096.
Morel, N., Dunant, Y., Israël, M., 2001. Neurotransmitter release through the V0 sector of V-ATPase. J. Neurochem. 79, 485–488.
Muller, D., Garcia-Segura, L.M., Parducz, A., Dunant, Y., 1987. Brief occurrence of a population of large intramembrane particles in the presynaptic membrane during transmission of a nerve impulse. Proc. Natl. Acad. Sci. USA 84, 590–594.
Nelson, N., Harvey, W.R., 1999. Vacuolar and plasma membrane proton-adenosinetriphosphatases. Physiol. Rev. 79, 361–385.
Ornstein, L.S., Zernike, F., 1914. Accidental deviations of density and opalescence at the critical point of a single sustance. Proc. Acad. Sci. Amst. 17, 793–806.
Park, J.M., Lubensky, T.C., 1996. Interactions between membrane inclusions on fluctuating membranes. J. Phys. I Fr. 6, 1217–1235.
Parri, H.R., Gould, T.M., Crunelli, V., 2001. Spontaneous astrocytic Ca2+ oscillations *in situ* drive NMDAR-mediated neuronal excitation. Nat. Neurosci. 4, 803–812.
Percus, J.K., Yevick, G.J., 1958. Analysis of classical statistical mechanics by means of collective coordinates. Phys. Rev. 110, 1–13.
Peters, C., Bayer, M.J., Bühler, S., Andersen, J.S., Mann, M., Mayer, A., 2001. Trans-complex formation by proteolipid channels in the terminal phase of membrane fusion. Nature 409, 581–588.
Smith, J.E., Reese, T.S., 1980. Use of aldehyde fixatives to determine the rate of synaptic transmitter release. J. Exp. Biol. 89, 19–29.
Takano, Y., Kamiya, H.O., 1979. Effect of ionic environment on densities of membrane-associated particles in presynaptic membranes observed in freeze-fractured synaptosomes. Experientia 35, 1076–1078.
Torri-Tarelli, F., Grohovaz, F., Fesce, R., Ceccarelli, B., 1985. Temporal coincidence between synaptic vesicle fusion and quantal secretion of acetylcholine. J. Cell Biol. 101, 1386–1399.
Verkleij, A.J., 1984. Lipid intramembranous particles. Biochim. Biophys. Acta. 779, 43–63.
Villegas, J., Jenden, D.J., 1979. Acetylcholine content of the Schwann cell and axon in the giant nerve fibre of the squid. J. Neurochem. 32, 761–766.

(*Accepted* 8 *March* 2002)